Received: 28 March 2021 | Revised: 18 April 2021 | Accepted: 04 May 2021
DOI: 10.22034/ecc.2021.278690.1154
Eurasian Chemical Communications
SAMI

FULL PAPER

The computational screening of structural, electronic, and optical properties for SiC, $Si_{0.94}Sn_{0.06}C$, and $Si_{0.88}Sn_{0.12}C$ lead-free photovoltaic inverters using DFT functional of first principle approach

Md. Hazrat Ali[a] |Mohammad Jahidul Islam[b,c,*] |Mostofa Rafid[a] |Razib Ahmed[a] |Md. Rakib Rayhan Jeetu[a] |Rinkan Roy[a] |Unesco Chakma[a] |Ajoy Kumer[d,e,*]

[a]*Department of Electrical and Electronics Engineering, European University of Bangladesh, Gabtoli, Dhaka-1216, Bangladesh*

[b]*Department of Physics, European University of Bangladesh, Gabtoli, Dhaka-1216, Bangladesh*

[c]*Department of Physics, Jagannath University, Dhaka-1100, Bangladesh*

[d]*Department of Chemistry, European University of Bangladesh, Gabtoli, Dhaka-1216, Bangladesh*

[e]*Department of Chemistry, Bangladesh University of Engineering and Technology, Dhaka-1000, Bangladesh*

***Corresponding Authors:**
Mohammad Jahidul Islam and Ajoy Kumer
Email: jahidulkhan106490@gmail.com and kumarajoy.cu@gmail.com
Tel.: +8801517149042 and +8801770568699

The structural, electronic, and optical nature for SiC, $Si_{0.94}Sn_{0.06}C$, and $Si_{0.88}Sn_{0.12}C$ lead-free photovoltaic inverters have been examined in this work for the first time using DFT based on CASTEP code. For developing the photovoltaic inverters, silicon carbide (SiC), was optimized by the DFT method of the computational tool using Generalized Gradient Approximation (GGA) based on the Perdew Burke Ernzerhof (PBE). The DOS and PDOS were calculated. It was obtained as a hexagonal geometry structure and its band gap was 2.3 eV as an indirect band gap which indicated the photovoltaic inverters. Afterward, the doping effect was recorded by using Sn metals at 6% and 12% replacing the Si atom. The band gaps for 6% and 12% of Sn doped were 2.00 eV and 1.65 eV, respectively, that provided the evidence as strong inverters in term of band gap. The optical properties, such as absorption, reflection, refractive index, conductivity, dielectric function, and loss function were calculated for SiC, $Si_{0.94}Sn_{0.06}C$, and $Si_{0.88}Sn_{0.12}C$. As a final remark, it can be said that the doping effect of 12% of Sn metals on silicon carbide (SiC) can reduce the band gap and supportive for photovoltaic inverters from optical properties.

KEYWORDS

Photovoltaic inverter; electronic structure; DOS; PDOS; optical properties.

Introduction

Semiconductor materials provide the great effect of sustainable energy for tremendous growth in solar technology due to produce an electronic device such as light emitting diodes (LEDs) [1], operating higher voltage or at high temperature in future. Most of the electronic technologies entirely depend on using of semiconductors [2]. The energy conversion of thermal to electrical energy from the sun is the adequate source available in the world. In several ways, solar energy can be helpful such as solar heating and photovoltaic (PV) [3-5]. This is why, there is great interest in using electrical semiconductor materials for higher thermal conductivity, lower production cost [6], including solar cell [7], higher current density [8], near visible, mid visible, deep visible light detections [9], and larger electric breakdown

strength [10] to build larger promising materials. The earth receives the renewable energy from the sun which can not entirely be converted and dispensed into electrical energy owing to lacking of efficiency from 15% to 17 % of silicon based solar cell [11]. For increasing their efficiency level, the modern multi-junction with concentrated photovoltaic (CPV) [12] applied for replacing silicon-based solar cells, providing reasonable capital investment for solar farms [13]. Due to the excellent behaviors, such as impactful physical properties [14], good chemical stability [15], environmental benign [16-20], sustainable energy [21] and interesting optical properties [22], semiconductors based on the quantum dot has been studied. So, developing semiconductor material with higher efficiency at room temperature is inevitable. Currently the transition metal ions like Ni, Sn, Cu, Fe etc. doped by II to IV group semiconductors such as ZnS, ZnO, CuO_2,CdS , and others, have drawn great attention [23-26].

In recent years, producing increment from regenerative energy sources was registered in the energy mixes of several development countries [27-29]. One of the great mature technologies from renewable energy sources like photovoltaic (PV) power systems consisting grid connected inverters are very popular in commercial domestic power plants [30, 31]. Nowadays, the lead-free SiC semiconductor has been widely used as an inverter in power electronics device [32] where energy from photovoltaic rays (PV) into an electrical grid is transferred and heat exchanger [33] happens in the solar power . In the photovoltaic energy conversion system, SiC semiconductor plays a significant role for removing various problems of the materials restriction of silicon. The silicon carbide semiconductor was used in the first photovoltaic inverter, as reported by Frank and Bruno [34]; currently metal oxide semiconductor field effect transistors, (MOSFETs) [35], junction field effect transistors (JFETs) [36], bipolar junction transistors (BJTs) [37] are available in the world. The aim of this research is to develop the photovoltaic inversion process after doping silicon carbide by transition metal atom of tin (Sn) for removing the barrier and improving the significant application for photovoltaic inverter system in future studies due to great effect of silicon carbide (SiC).

This paper covers the comparative study of SiC including the investigation of structural, electronic, and optical properties using the first principle method based on the density functional theory (DFT). The novelty of this research lies in the base material silicon carbide (SiC) doped by 6% and 12% of Sn atom and various properties have been studied for the first time. As the most accurate method GGA with PBE has been used for determining the electronic and optical properties with the same setting option for SiC, $Si_{0.94}Sn_{0.06}C$, and $Si_{0.88}Sn_{0.12}C$ crystals for its vast applications [17, 38-43].

Computational methods

The method of GGA with PBE was executed [44] from CASTEP code from material studio 8.0 [45] for calculating the electronic structure for crystals. Firstly, the structural optimization for SiC crystal was performed by GGA with PBE method. For simulation, the convergence criterion for the force between atoms was 2×10^{-6} eV/atom, 1×10^{-5} Å as the maximum displacement and 1×10^{-5} eV/atom as the total energy, and the same condition was applied for SiC, $Si_{0.94}Sn_{0.06}C$, and $Si_{0.88}Sn_{0.12}C$ keeping the cut off at 523, and k point at 4×4×2 with norm-conserving pseudo potentials functional. The 2×1×1 supercell models were considered to simulate the optimized material for calculating structural and electronic properties [43]. Then, the density of states (partial or total) and optical properties were calculated with same condition.

Results and discussion

Optimized structure

The lattice constant values for SiC, $Si_{0.94}Sn_{0.06}C$ and $Si_{0.88}Sn_{0.12}C$ are evaluated from the materials studio after optimizing their crystal structure. It was illustrated that the tetragonal type, space group P63mc [186] was selected for computational study which represented the similar value of experimental data as shown in Table 01. The optimized structure of materials is shown in Figure 1, which was taken after simulation GGA with PBE which is considered as the standard functional of DFT having heavy metal atoms in crystal.

TABLE 1 Structural calculation by GGA with PBE method

Compound	a	b	C	α	β	γ	Crystal type	Space group	Density
SiC	3.094 Å	3.094 Å	10.128 Å	90.00°	90.00 °	120.00 °	hexagonal	P63mc [186]	3.17 g/cm³
$Si_{0.94}Sn_{0.06}C$	3.094 Å	3.094 Å	10.128 Å	90.00°	90.00 °	120.00 °	hexagonal	P63mc [186]	3.17 g/cm³
$Si_{0.88}Sn_{0.12}C$	3.094 Å	3.094 Å	10.128 Å	90.00°	90.00 °	120.00 °	hexagonal	P63mc [186]	3.17 g/cm³

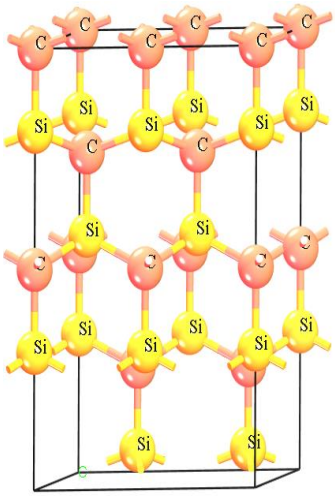

FIGURE 1(a) Optimized structure for SiC

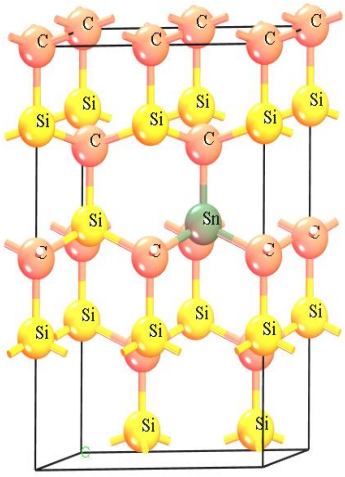

FIGURE 1(b) Optimized structure for $Si_{0.94}Sn_{0.06}C$

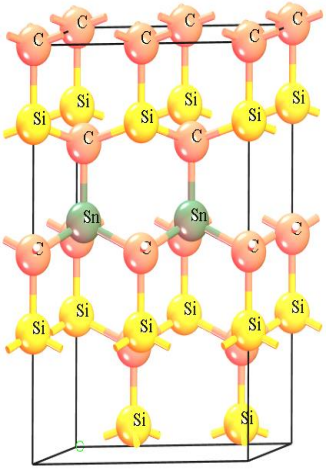

FIGURE 1(c) Optimized structure for $Si_{0.88}Sn_{0.12}C$

Electronic structure

The electronic energy gap has been used to calculate the electronic properties of SiC, $Si_{0.94}Sn_{0.06}C$, and $Si_{0.88}Sn_{0.12}C$. The band gap between the highest energy state of the valence band and the lowest energy state of the conduction band is closely related to the LUMO-HOMO gap. The Fermi energy level between the conduction and valence band was set at 0 eV. Based on the energy band, crystal materials have either indirect band gap or direct band gap. As shown in Figure 2(a), it was observed that the momentum of the minimum energy state of the conduction band was found in the Q point and the maximum energy state of the valence band was obtained in different G symmetry points. So, electron cannot shift the highest energy state of the valence band to the lowest energy state of the conduction band without change in momentum. The calculated band gap was found at 2.30 eV for SiC shown in Figure 2(a). After doping by 6%, the electronic band gap declined, which is reported 2.0 eV for $Si_{0.94}Sn_{0.06}C$ is shown in Figure 2(b). From Figure 2(c), having 12% dope of Sn with Si atom the band gap reduced by 0.65 eV and observed 1.65 eV for $Si_{0.88}Sn_{0.12}C$. It can be

seen that both materials following indirect band gap due to MCB and MVB are at different points of symmetry. Owing to indirect band gap, so that this semiconductor does not absorb light well this is important fact for photovoltaic or solar cell. The values of electronic band gaps for SiC, $Si_{0.94}Sn_{0.06}C$, and $Si_{0.88}Sn_{0.12}C$ semiconductors are listed in Table 2.

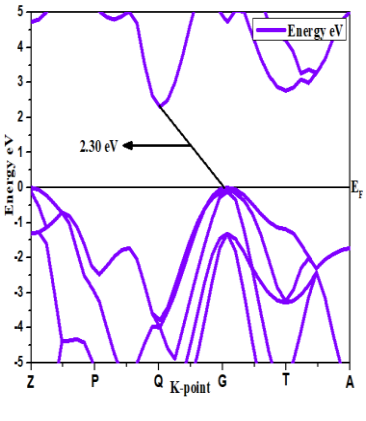

FIGURE 2(a) Electronic structure for SiC

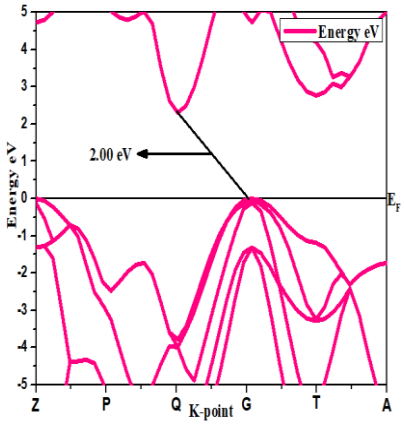

FIGURE 2(b) Electronic structure for $Si_{0.94}Sn_{0.06}C$

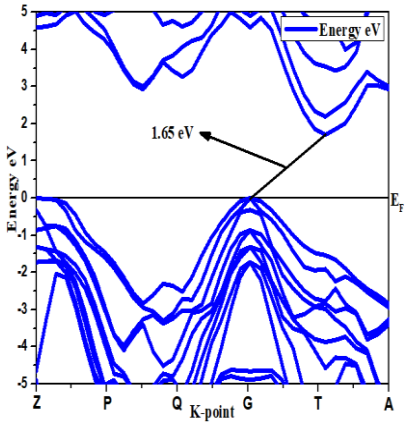

FIGURE 2(c) Electronic structure for $Si_{0.88}Sn_{0.12}C$

TABLE 2 Band gaps for SiC, $Si_{0.94}Sn_{0.06}C$, and $Si_{0.88}Sn_{0.12}C$

Compound	Method of GGA with PBE	Experimental value
SiC	**2.30**	**2.22**
$Si_{0.94}Sn_{0.06}C$	2.00	Newly predicted
$Si_{0.88}Sn_{0.12}C$	1.65	Newly predicted

Density of states and partial density of states

In order to reveal the electronic band structure and scattering of an orbital of materials, the density of state or partial density of states plays a significant role. For an energy interval, density of states is discontinuous which states that in the band gap region no states found for electron occupies of the materials. The method GGA with PBE has been used to interpret DOS and PDOS of Si, C, and Sn atoms for SiC, $Si_{0.94}Sn_{0.06}C$, and $Si_{0.88}Sn_{0.12}C$ crystal materials. Density of states upper Fermi level energy illustrates the Lowest Unoccupied Molecular Orbital (LUMO) and negative part of photon energy represents the Highest Occupied Molecular Orbital (HOMO) as shown in Figure 3(a) to 3(l). Figure 3(a) depicts the comparative study of DOS for SiC, $Si_{0.94}Sn_{0.06}C$, and $Si_{0.88}Sn_{0.12}C$ which explains the maximum electron density of valence band and conduction band for $Si_{0.88}Sn_{0.12}C$ than SiC and $Si_{0.94}Sn_{0.06}C$ crystal. Figure 3(b) represents the PDOS for SiC crystal consists of $3p^2$ for Si atom and $2p^2$ for C element. The strong hybridization occurs for p orbital of C atom in valence band and p orbital of Si atom in conduction band for SiC. The PDOS for $Si_{0.94}Sn_{0.06}C$ semiconductor consists of $3p^2$ for Si atom, $2p^2$ for C atom and $5p^2$ for Sn atom which can be seen in Figure 3(c). The p orbital of C atom provides strong contribution for valence band and p orbital of Si and Sn atoms provide higher contribution for conduction band. Figure 3(d) depicts the PDOS, consisting of $3p^2$ for Si atom, $2p^2$ for C atom and $5p^2$ for Sn atom. Figures 3(e) to 3(l) depict the comparative study of s, p, and d orbital's for SiC, $Si_{0.94}Sn_{0.06}C$, and $Si_{0.88}Sn_{0.12}C$. From the study, it can be said that the p orbital is the higher contributor of both conduction bands for $Si_{0.94}Sn_{0.06}C$ and $Si_{0.88}Sn_{0.12}C$ crystals.

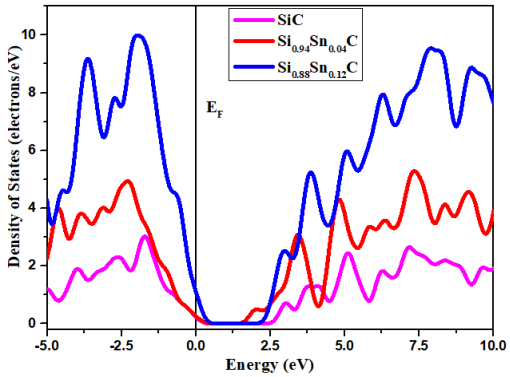

FIGURE 3(a) Comparison of total DOS for doped and undoped

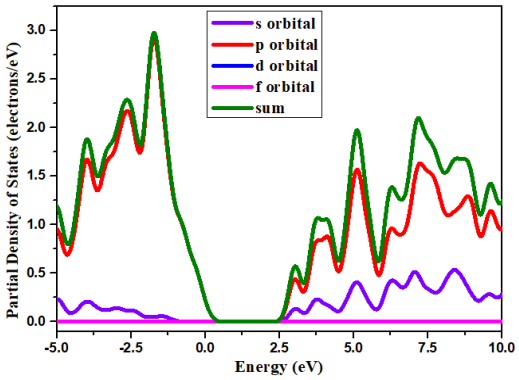

FIGURE 3(b) PDOS for undoped

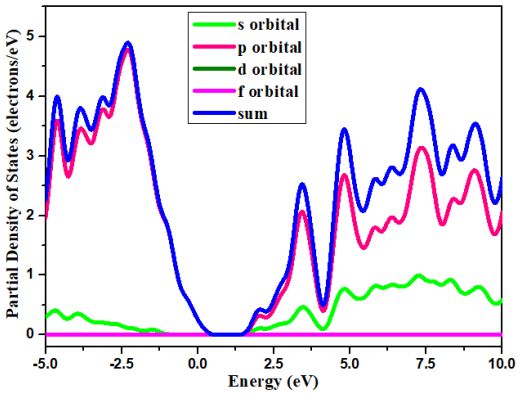

FIGURE 3(c) PDOS for $Si_{0.94}Sn_{0.06}C$

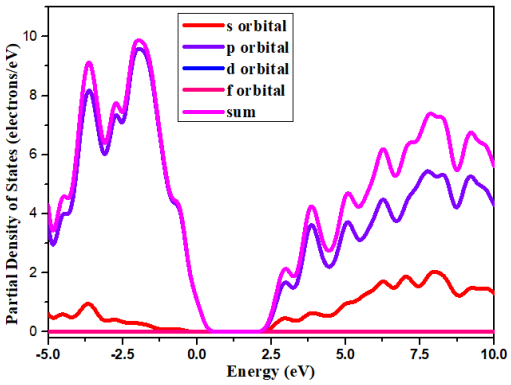

FIGURE 3(d) PDOS for $Si_{0.88}Sn_{0.12}C$

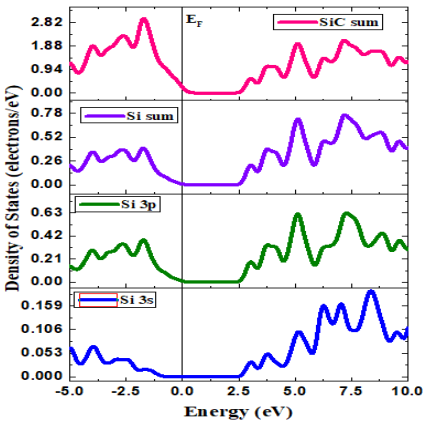

FIGURE 3(e) PDOS SiC for Si atom

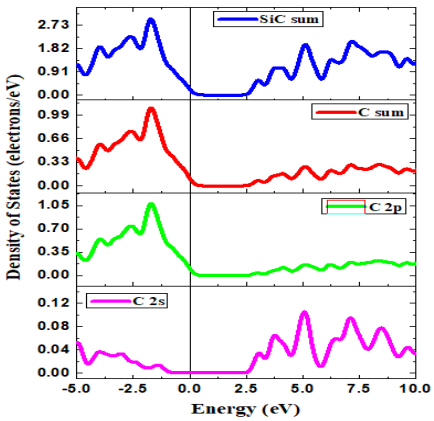

FIGURE 3(f) PDOS SiC for C atom

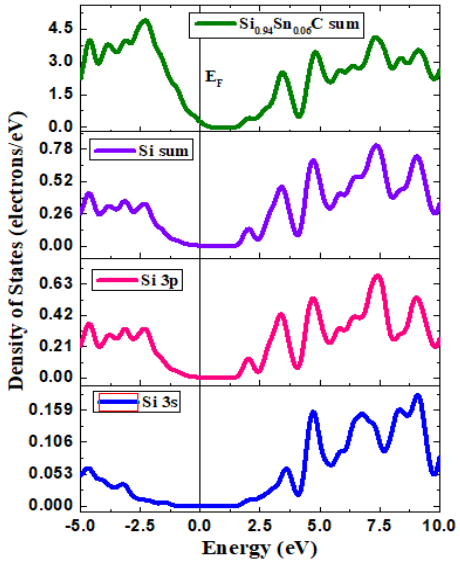

FIGURE 3(g) PDOS in $Si_{0.94}Sn_{0.06}C$ for Si atom

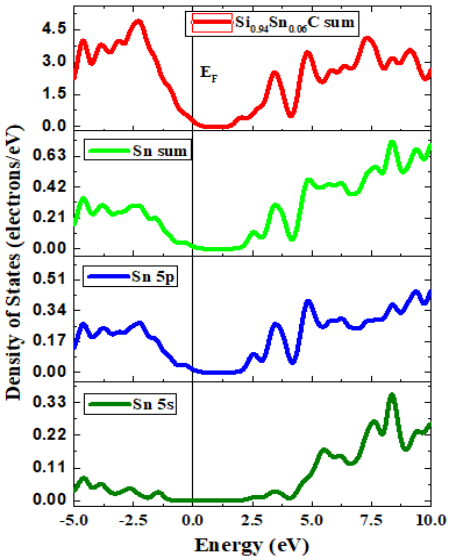

FIGURE 3(h) PDOS in $Si_{0.94}Sn_{0.06}C$ for Sn atom

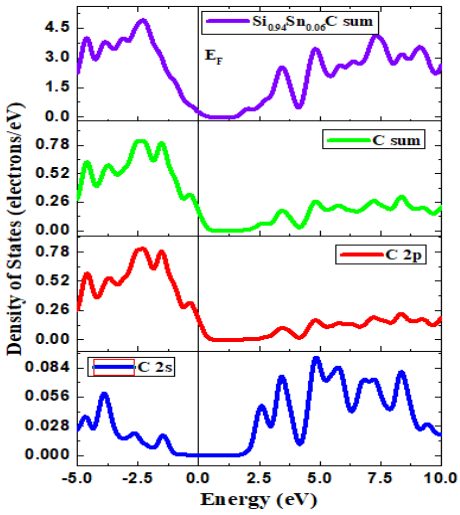

FIGURE 3(i) PDOS in $Si_{0.94}Sn_{0.06}C$ for C atom

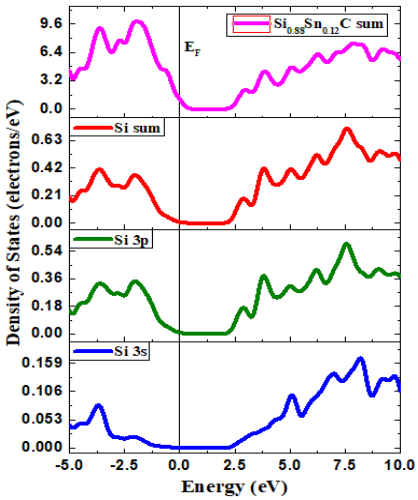

FIGURE 3(j) PDOS in $Si_{0.88}Sn_{0.12}C$ for Si atom

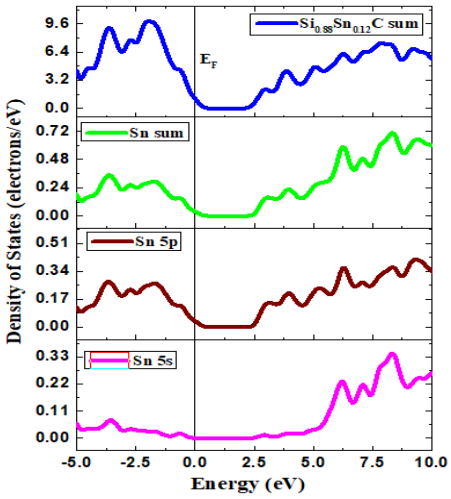

FIGURE 3(k). PDOS in $Si_{0.88}Sn_{0.12}C$ for Sn atom

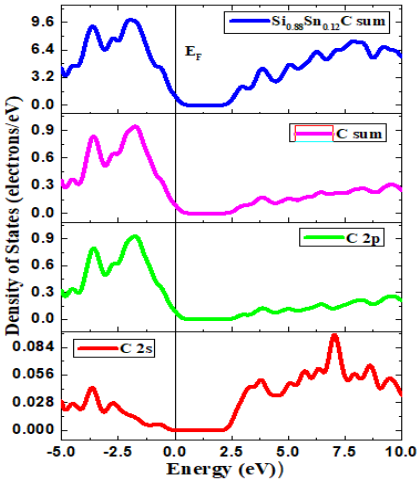

FIGURE 3(l) PDOS in $Si_{0.88}Sn_{0.12}C$ for C atom

Optical properties

Optical reflectivity

Reflectivity is a significant optical property of semiconducting material in which the amount of light that is incident on the surface of the semiconductor material can be estimated from the reflectivity data which is related to the absorbance of that material. It is noted that a smaller value of reflectivity shows greater absorption of light or UV. In this research, the reflectivity of SiC, $Si_{0.94}Sn_{0.06}C$, and $Si_{0.88}Sn_{0.12}C$ crystal was observed, respectively shown in Figure 4. The value of reflectivity near photon energy 0 eV is around 0.2, which represents no band gap found in the Fermi energy level that confirms SiC, $Si_{0.94}Sn_{0.06}C$, and $Si_{0.88}Sn_{0.12}C$ have a semi-conductor nature. It is found that the values of reflectivity for SiC, $Si_{0.94}Sn_{0.06}C$, and $Si_{0.88}Sn_{0.12}C$ remain the same in the photon energy range between 0 eV to 1.5 eV is about 0.22. Above energy 1.5 eV, the reflectivity increases moderately after 12% doping of Sn atom with Si for $Si_{0.88}Sn_{0.12}C$ material than SiC and $Si_{0.94}Sn_{0.06}C$ materials.

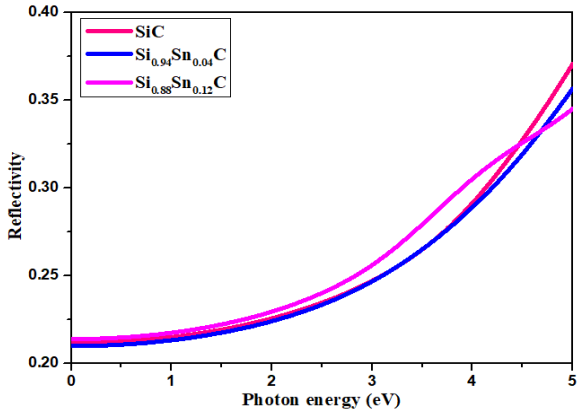

FIGURE 4. Reflectivity

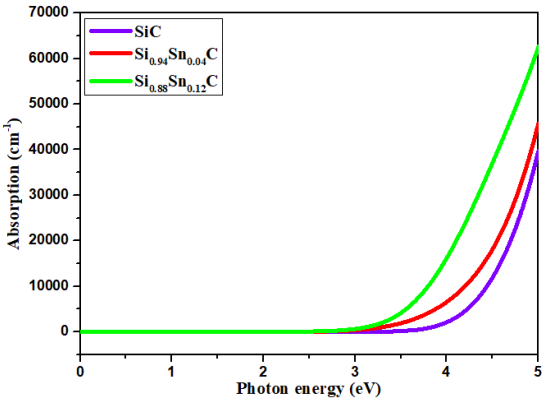

FIGURE 5. Absorption

Absorption

The absorption spectrum of a material depends on the nature of the energy band gap which follows the indirect band gap usually absorbs more temperature than the direct band gap semiconductor, because there are fewer phonons at low temperature. For indirect band gap semiconductor, the light with photon energy near to the band gap can attenuate much before being absorbed than direct band in previous investigation [46, 47]. Figure 5 illustrates comparative study of the absorption for SiC, $Si_{0.94}Sn_{0.06}C$, and $Si_{0.88}Sn_{0.12}C$. The polycrystalline polarization technique and the electrical field vector as an isotropic average were used to determine the optical absorption of SiC, $Si_{0.94}Sn_{0.06}C$, and $Si_{0.88}Sn_{0.12}C$ semiconductor. It is revealed that absorption peaks are attributed to the transition of energy from highest energy states of valence band to the lowest energy state of conduction band under UV or visible light illumination that indicates materials can absorbs photons of visible range. From the photon energy level 0 to 3.5 eV, the absorption of all three materials remains the same and then absorption increases rapidly for $Si_{0.88}Sn_{0.12}C$ and $Si_{0.94}Sn_{0.06}C$ but for undoped material rises moderately after 4 eV. So, it can be said that the semiconductor doping by 12% of Sn with Si of SiC can absorb larger visible light than other materials SiC and $Si_{0.94}Sn_{0.06}C$. Due to the maximum absorption found for $Si_{0.88}Sn_{0.12}C$ semiconductor in the mid visible range 3.94 eV to 4.43 eV and deep visible range above 4.43 eV, it is a good absorber in that region.

Refractive index

The refractive index or index of refraction is a significant parameter for measuring the characteristics of materials that reveals how fast visible light travels through the material. In previous investigation, it was reported that higher value of refractive index is associated with the larger and denser medium of material [48]. The refractive index has two segments: Real portion and imaginary portion. The real part of refractive index indicates the phase velocity whereas the imaginary segment is mass attenuation coefficient. Figure 6 depicts the comparative study of refractive index as a function of photon energy reveals that the values for the imaginary part are almost zero until photon energy 3.5 eV for SiC, $Si_{0.94}Sn_{0.06}C$, and $Si_{0.88}Sn_{0.12}C$ materials, whereas at initial point of photon energy, the value of refractive index is at around 2.7 for real part of both doped and undoped semiconductor. Above photon energy 2.5 eV, the values of the refractive index of the real segment change in a similar trend for SiC, $Si_{0.94}Sn_{0.06}C$, and $Si_{0.88}Sn_{0.12}C$.

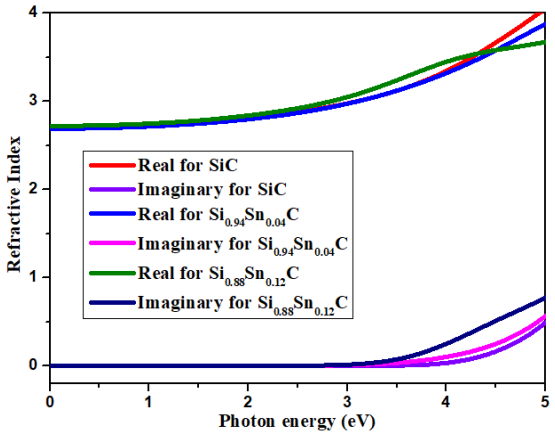

FIGURE 6 Refractive Index

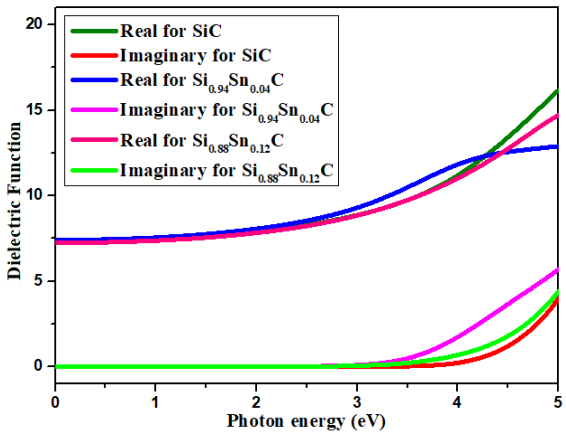

FIGURE 7 Dielectric function

Dielectric function

The dielectric function or relative permittivity is important tool to investigate their optical properties which is related with adsorption properties as the following equation revels for solid [49, 50].

$$\varepsilon = \varepsilon_1(\omega) + i\varepsilon_2(\omega)$$

Here, $\varepsilon_1(\omega)$, and $\varepsilon_1(\omega)$ denotes the dielectric constant (real part) and the dielectric loss factor (imaginary part), respectively. The band structure of any material is the probability of photon absorption, which is closely related to the imaginary segment of dielectric function. The real part of the dielectric function shows the energy storing capacity and the energy attenuation capability for nonconductor materials. It can be seen from figure 7, the dielectric function initiated from 7.5 for real part of doped and undoped material at 0 eV and changes steadily with changing photon energy at around 3 eV. However, the imaginary part shows zero dielectric function up to 3.5 eV for SiC, $Si_{0.94}Sn_{0.06}C$, and $Si_{0.88}Sn_{0.12}C$ materials, and above that dielectric function increases rapidly for $Si_{0.94}Sn_{0.06}C$.

Conductivity

The optical conductivity of the semiconductor on the basis of the energy band and free electrons is linked with the discrete space of electrons in orbit. This is also produced due to the presence of holes and free electrons in the crystal molecules. Figure 8 represents the optical conductivity changes with rising photon energy for SiC, $Si_{0.94}Sn_{0.06}C$, and $Si_{0.88}Sn_{0.12}C$. It can be seen that the value of the imaginary part of conductivity decreases

exponentially with changing photon energy for both doped and undoped material even that the initial value was zero at 0 eV. However, the optical conductivity value was almost same up to photon energy 3.5 eV for real part of both doped and undoped semiconductors.

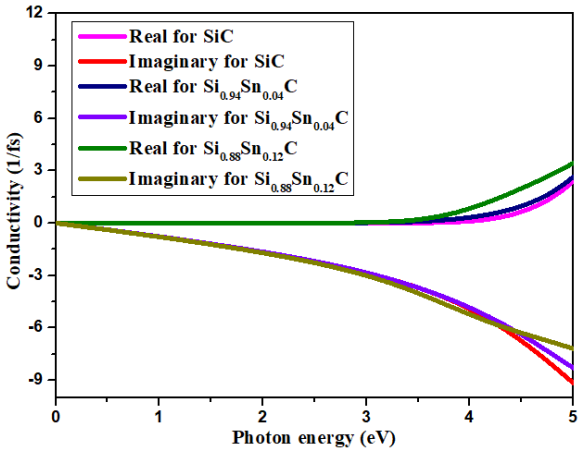

FIGURE 8 Conductivity

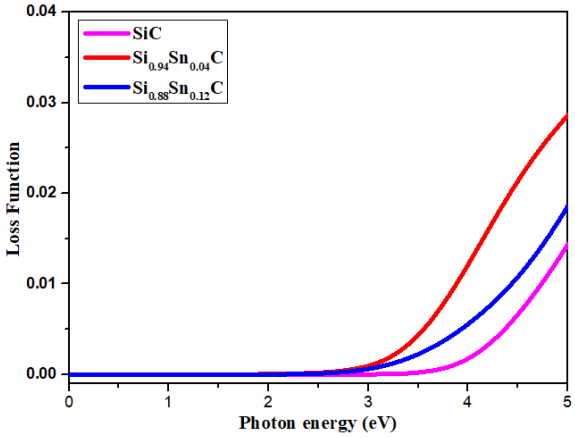

FIGURE 9 Loss function

Loss function

There are two segments for electronic energy loss function such as high energy region and low energy region for the optical properties. The high energy portion follows the higher loss function and the opposite is the lower energy loss function. The energy loss function is closely related to the dielectric constant of the materials in the range of the dielectric theory validation. Figure 9 shows the comparative study of loss function as a function of photon energy for SiC, $Si_{0.94}Sn_{0.06}C$, and $Si_{0.88}Sn_{0.12}C$. It can be seen that up to photon energy 3 eV no loss function was found for SiC, $Si_{0.94}Sn_{0.06}C$, and $Si_{0.88}Sn_{0.12}C$ semiconductors and then loss function enhanced rapidly for $Si_{0.94}Sn_{0.06}C$ with rising photon energy. However, the loss function of SiC and $Si_{0.88}Sn_{0.12}C$ rises slowly due to increasing energy.

Conclusion

To sum up, the electronic, structural, and optical properties of hexagonal SiC, $Si_{0.94}Sn_{0.06}C$, and $Si_{0.88}Sn_{0.12}C$ lead-free photovoltaic inverters have been studied for the first time using the DFT functional by first principle approach. The electronic band gaps have been recorded for SiC, $Si_{0.94}Sn_{0.06}C$, and $Si_{0.88}Sn_{0.12}C$ are 2.30 eV, 2.0 eV and 1.65 eV by GGA with PBE showing more consistency with the experimental value 2.22 eV for SiC. After 12% Sn doping in silicon carbide (SiC) the band gap reached 1.65 eV which is important for improving photovoltaic inverter system. The photon energy is dependent on optical properties such as optical reflectivity, absorption, refractive index, conductivity, dielectric function, and loss function that have been investigated and explained broadly. It has revealed that $Si_{0.88}Sn_{0.12}C$ is a good absorber in the higher photon energy and a good reflector in deep visible range of light. The density of states and partial density of states have been investigated for SiC, $Si_{0.94}Sn_{0.06}C$, and $Si_{0.88}Sn_{0.12}C$ photovoltaic inverters.

Acknowledgements

I am thankful to my professor Dr. Parimal Bala and Dr. Kamrul Alam Khan, Department of Physics, Jagannath University, Dhaka, Bangladesh for inspiration to carry on my research.

Funding:

Authors confirm that there is no funding from any institution or university.

Orcid:
Mohammad Jahidul Islam: https://www.orcid.org/0000-0002-4125-8222
Unesco Chakma: https://www.orcid.org/0000-0003-1711-7216
Ajoy Kumer: https://www.orcid.org/0000-0001-5136-6166

References

[1] B.K. SaifAddin, A.S. Abdullah, C.J. Zollner, F. Wu, B. Bonef, M. Iza, S. Nakamura, S.P. DenBaars, J.S. Speck, *ACS Photonics,* **2020**, *7*, 554-561. [crossref], [Google Scholar], [Publisher]
[2] E. Vogel, *Nat. Nanotechnol*., **2007**, *2*, 25-32. [crossref], [Google Scholar], [Publisher]
[3] C.N.M. Ho, H. Breuninger, S. Pettersson, G. Escobar, F. Canales, *IEEE Trans. Power Electron.,* **2012**, *28*, 289-299. [crossref], [Google Scholar], [Publisher]
[4] A. Kumer, B. Ahmed, Md.A. Sharif, Abdullah Al-Mamun, *Asian J. Phys. Chem. Sci,* **2017**, *4*, 1-12. [crossref], [Google Scholar], [Publisher]
[5] A.H.S. Al-Waeli, K. Sopian; M.T. Chaichan, H.A. Kazem, H.A.R. Hasan, A.N. Al-Shamani, *Energy Convers. Manag.,* **2017**, *142*, 547-558. [crossref], [Google Scholar], [Publisher]
[6] B. Babić, D. Bučevac, A. Radosavljević-Mihajlović, A. Došen, J. Zagorac, J. Pantić, B. Matović, *J. Eur. Ceram. Soc.,* **2012**, *32*, 1901-1906. [crossref], [Google Scholar], [Publisher]
[7] H. Heidarzadeh, A. Rostami, M. Dolatyari, *MAT SCI SEMICON PROC,* **2020**, *109*, 104936. [crossref], [Google Scholar], [Publisher]
[8] H. Luo, F. Iannuzzo, N. Baker, F. Blaabjerg, W. Li, X. He, *IEEE Trans. Emerg. Sel. Topics Power Electron,* **2019**, *8*, 1622-1632. [crossref], [Google Scholar], [Publisher]
[9] M.Q. Li, N. Yang; G.G. Wang, H.Y. Zang, J.C. Han, *Appl. Surf. Sci.,* **2019**, *471*, 694-702. [crossref], [Google Scholar], [Publisher]
[10] Y. Feng, B. Miao, Gong, Y. Xie, X. Wei, Z. Zhang, *ACS Appl. Mater. Interfaces,* **2016**, *8*, 19054-19065. [crossref], [Google Scholar], [Publisher]
[11] H. Heidarzadeh, H. Baghban, H. Rasooli, M. Dolatyari, A. Rostami, *Optik,* **2014**, *125*, 1292-1296. [crossref], [Google Scholar], [Publisher]
[12] M. George, A.K. Pandey, N.A. Rahim, V.V. Tyagi, S. Shahabuddin, R. Saidur, *Energy Convers. Manag.,* **2019**, *186*, 15-41. [crossref], [Google Scholar], [Publisher]
[13] B.N. Pushpakaran, A.S. Subburaj, S.B. Bayne, J. Mookken, *Renewable Sustainable Energy Rev.,* **2016**, *55*, 971-989. [crossref], [Google Scholar], [Publisher]
[14] K.A. Terrani, Y. Yang, Y-J. Kim, R. Rebak, H.M. Meyer III, T.J. Gerczak, *J. Nucl. Mater,* **2015**, *465*, 488-498. [crossref], [Google Scholar], [Publisher]
[15] K.L. Choy, *Scripta Metallurgica et Materialia,* **1995**, *32*, 219-224. [crossref], [Google Scholar], [Publisher]
[16] I. Spitsberg, J. Steibel, *Int. J. Appl. Ceram. Technol.,* **2004**, *1*, 291-301. [crossref], [Google Scholar], [Publisher]
[17] M.M. Hasan, A. Kumer, U. Chakma, M.T. Islam, *Molecular Simulation,* **2021**, *47*, 1-13. [crossref], [Google Scholar], [Publisher]
[18] M.J. Islam, A. Kumer, *SN Applied Sciences,* **2020**, *2*, 251. [crossref], [Google Scholar], [Publisher]
[19] M.B. Ahmed, A. Kumer, M. Islam, T.S.A. Islam, *J. Turkish Chem. Soc., Section A: Chemistry,* **2018**, *5*, 803-818. [crossref], [Google Scholar], [Publisher]
[20] M.I. Hossain, A. Kumer, S.H. Begum, *Asian J. Chem. Sci.,* **2018**, *5*, 1-9. [crossref], [Google Scholar], [Publisher]
[21] S.M. Kim, P.S. Ihl. Woo, *ChemSusChem,* **2012**, *5*, 1513-1522. [crossref], [Google Scholar], [Publisher]
[22] H.C. Hsueh, G.Y. Guo, S.G. Louie, *Phys. Rev. B,* **2011**, *84*, 085404. [crossref], [Google Scholar], [Publisher]

[23] N. Chen, Y. Hu, X. Liu, J. Yang, W. Li, D. Lu, J. Fu, Y. Liang, W. Wang, *J. Phys. Chem. C*, **2020**, *124*, 21968-21977. [crossref], [Google Scholar], [Publisher]
[24] T.F. Khan, M. Muhyuddin, S.W. Husain, M.A. Basit, *16th International Bhurban Conference on Applied Sciences and Technology (IBCAST)*, **2019**, 60-65. [crossref], [Google Scholar], [Publisher]
[25] N.N. Omrani, A.N. Ejhieh, *Sep. Purif. Technol.,* **2020**, 235, 116228. [crossref], [Google Scholar], [Publisher]
[26] M.T. Islam, A. Kumer, U. Chakma, D. Howlader, *Orbital: Electron. J. Chem.,* **2021**, *13*. [crossref], [Google Scholar], [Publisher]
[27] T.J. Hammons, *Int. J. Electr. Power Energy Syst.,* **2008**, *30*, 462-475. [crossref], [Google Scholar], [Publisher]
[28] I. Dincer, *Renewable Sustainable Energy Rev.,* **2000**, *4*, 157-175. [crossref], [Google Scholar], [Publisher]
[29] M.A. Eltawil, Z. Zhengming, L. Yuan, *Renewable Sustainable Energy Rev.,* **2009**, *13*, 2245-2262. [crossref], [Google Scholar], [Publisher]
[30] D. Barater, C. Concari, G. Buticchi, E. Gurpinar, D. De, A. Castellazzi, *IEEE Trans. Ind. Appl.,* **2016**, *52*, 2475-2485. [crossref], [Google Scholar], [Publisher]
[31] E. Gurpinar, D. De, A. Castellazzi, D. Barater, G. Buticchi, G. Francheschini, *IEEE 15th Workshop on Control and Modeling for Power Electronics (COMPEL)*, **2014**, 1-7. [crossref], [Google Scholar], [Publisher]
[32] D. Han, Y. Li, B. Sarlioglu, *IEEE Applied Power Electronics Conference and Exposition (APEC)*, **2015**, 304-310. [crossref], [Google Scholar], [Publisher]
[33] X. Li, J. Song, G. Yu, Y. Liang, H. Tian, G. Shu, C.N. Markides, *Energy Convers. Manag.,* **2019**, *199*, 111968. [crossref], [Google Scholar], [Publisher]
[34] Y. Ando, T. Oku, M. Yasuda, Y. Shirahata, K. Ushijima, M. Murozono, *Sol. Energy,* **2017**, *141*, 228-235. [crossref], [Google Scholar], [Publisher]
[35] B. Hull, S. Allen, Q, Zhang, D. Gajewski, V. Pala, J.Richmond, S. Ryu, M. O'Loughlin, E.V. Brunt, L. Cheng, A. Burk, J. Casady, D. Grider, J. Palmour, in *2014 IEEE Workshop on Wide Bandgap Power Devices and Applications*, **2014**, 139-142. [crossref], [Google Scholar], [Publisher]
[36] S. Bellone, L.D. Benedetto, G.D. Licciardo, *Solid-State Electronics,* **2015**, *109*, 17-24. [crossref], [Google Scholar], [Publisher]
[37] H. Elahipanah, S. Kargarrazi, A. Salemi, M. Östling, C.M. Zetterling, *IEEE Electron Device Letters,* **2017**, *38*, 1429-1432. [crossref], [Google Scholar], [Publisher]
[38] U. Chakma, A. Kumer, K.B. Chakma, M.T. Islam, D. Howlader, R.M.K. Mohamed, *Eurasian Chem. Commun.,* **2020**, *2*, 573-580. [crossref], [Google Scholar], [Publisher]
[39] U. Chakma, A. Kumer, K.B. Chakma, M.T. Islam, D. Howlader, *Adv. J. Chem. A,* **2020**, 542–550. [crossref], [Google Scholar], [Publisher]
[40] M.M. Hasan, A. Kumer, U. Chakma, *Adv. J. Chem. A,* **2020**, *03*, 639–644. [crossref], [Google Scholar], [Publisher]
[41] M.T. Islam, A. Kumer, D. Howlder, K.B. Chakma,, U. Chakma, *Turkish Computational and Theoretical Chemistry,* **2020**, *4*, 24-31. [crossref], [Google Scholar], [Publisher]
[42] K.B. Chakma. A. Kumer, U. Chakma, D. Howlader, M.T. Islam, *Int. J. New. Chem.,* **2020**, *7*, 247-255. [crossref], [Google Scholar], [Publisher]
[43] M.A.M. Sikder, U. Chakma, A. Kumer, M.J. Islam, A. Habib, M.M. Alam, *Appl. J. Environ. Eng. Sci.,* **2021**, 7, 103-113. [crossref], [Google Scholar], [Publisher]
[44] J.M. del Campo, J.L. Gazquez, S.B. Trickey, A. Vela, *J. Chem. Phys.,* **2012**, *136*, 104108. [crossref], [Google Scholar], [Publisher]
[45] J. Ramos, *Webinar Digitalización del Laboratorio Químico,* 27-Marzo-**2020**. [crossref], [Google Scholar], [Publisher]
[46] A.G. Bhuiyan, K. Sugita; K. Kasashima, A. Hashimoto, *Appl. Phys. Lett.,* **2003**, *83*,

4788-4790. [crossref], [Google Scholar], [Publisher]
[47] E. Davis, N. Mott, *Philosophical Magazine,* **1970**, *22*, 0903-0922. [crossref], [Google Scholar], [Publisher]
[48] F.P. Bolin, L.E. Preuss, R.C. Taylor, R.J. Ference, *Applied optics,* **1989**, *28*, 2297-2303. [crossref], [Google Scholar], [Publisher]
[49] D.A. Kleinman, *Phys. Rev.,* **1962**, *126*, 1977. [crossref], [Google Scholar], [Publisher]
[50] R. Lovell, *J. Phys. C: Solid State Phys.* **1974**, *7*, 4378. [crossref], [Google Scholar], [Publisher]

How to cite this article: Md. Hazrat Ali, Mohammad Jahidul Islam*, Mostofa Rafid, Razib Ahmed, Md. Rakib Rayhan Jeetu, Rinkan Roy, Unesco Chakma, Ajoy Kumer*. The computational screening of structural, electronic, and optical properties for SiC, $Si_{0.94}Sn_{0.06}C$, and $Si_{0.88}Sn_{0.12}$ C lead-free photovoltaic inverters using DFT functional of first principle approach**.** *Eurasian Chemical Communications*, 2021, 3(5), 327-338. **Link:** http://www.echemcom.com/article_130077.html